Evaluation of a Novel Maghemite Hybrid Nanocarrier for MR Imaging (Pilot Study)

[1]A. Malá, [2]A. Bakandritsos, [1]O. Macíček, [2]E. Rousalis, [1]E. Dražanová, [1]R. Jiřík, [1]L. Dvořáková, [1]L. Grossová, [1]Z. Starčuk jr.

[1]ASCR, Institute of Scientific Instruments, Brno, Czech Republic
[2]Department of Materials Science, University of Patras, Rion, Greece
Email: malaa@isibrno.cz

Abstract. *The aim of this study was to investigate Mag 102-6, a maghemite hybrid drug nanocarrier, as a potential T_2 contrast agent (CA) for magnetic resonance imaging (MRI). Samples of agar gel mixed with different Fe concentrations of Mag 102-6 were measured at laboratory temperature for relaxivity r_2 determination in 9.4 T. The results were compared with commercial CA FeraSpin XXL measured in the same arrangement. In addition, the r_2 of Mag 102-6 in saline solution at physiological temperature 37.7°C was measured. MRI was performed with four mice using a 9.4T NMR scanner before, and up to 24 h post-injection (p.i.) of Mag 102-6 (dose 5 mg Fe kg^{-1}). Images of abdomen were continuously acquired by segmented Multi Gradient Echo (MGE) pulse sequence from 1 minute before the CA application to 20 minutes p.i. The T_1-weighted (T_1-w) and T_2-weighted (T_2-w) images were captured before the application and 25 minutes, 3.5, 7 and 24 hours after CA application. R_2* changes in time were estimated from MGE images for various anatomical regions (kidney, muscles, liver) by fitting of signal intensities. Mag 102-6 and FeraSpin XXL had comparable r_2 values. Mag 102-6 showed the potential to be monitored by MRI as a T_2 CA.*

Keywords: Nanocarrier, Maghemite, Contrast Agent, MRI, r_2

1. Introduction

The connection of therapeutics and diagnostics into one "theranostic" assembly enables monitoring of drug circulation. Controlling the drug distribution is important for appropriate disease treatment. The most important phenomenon that enables magnetic resonance imaging to provide high contrast of soft tissues, revealing anatomic and physiologic information, are the relaxation processes of hydrogen protons as they proceed at the magnetic field of the scanner. By shortening relaxation times (T_1, T_2), MRI contrast agent particles modify proton signal intensities around themselves. The ability of a CA to increase the longitudinal relaxation rate R_1 (=1/T_1) or the transverse relaxation rate R_2 (=1/T_2), which both depend linearly on the CA concentration, expressed per millimolar concentration of agent, is the longitudinal relaxivity r_1 or transverse relaxivity r_2 [s^{-1} mM^{-1}]. Maghemite nanoparticles act as a T_2 contrast agent – their presence decreases the MRI signal intensity. The first step for the evaluation of CA characteristics was in vitro measurement of r_2 (in conditions ideally close to physiologic) and comparison with a similar commercial CA. The second step was in vivo measurement involving monitoring of the changes in signal intensity for different tissues and checking the tolerance of the CA bolus by animals.

2. Subject and Methods

Mag 102-6 as Contrast Agent

Hybrid magnetic drug nanocarrier Mag 102-6 consisted of a graft-type copolymer, poly(methacrylic acid)-graft-poly(ethylenglycol methacrylate), (p(MAA-g-EGMA)), which acts as a corona for magnetic iron oxide nanocrystals. Mag 102-6 combines bio-repellent

properties, high magnetic response and excellent loading capacity for anticancer drug doxorubicin [1]. Its mean hydrodynamic diameter (D_h) was 52 nm. Mag 102-6 without doxorubicin loading was used for whole study.

In Vitro Measurements

Six samples of saline (Isotonic Saline Solution 0.9%, Braun, Germany) mixed with Mag 102-6 with concentrations of 0, 0.02, 0.05, 0.10, 0.19 and 0.37 mM Fe were measured at laboratory temperature and at 37°C. Six samples of 1.5% agar gel mixed with 150 µL of Mag 102-6 with concentrations of 0, 0.02, 0.04, 0.09, 0.13 and 0.33 mM and, for comparison, a commercial contrast agent for preclinical applications, FeraSpin XXL (Miltenyi Biotec, Bergisch Gladbach, Germany), with D_h = 60-70 nm, in 1.5% agar gel at concentrations 0, 0.02, 0.04, 0.08, 0.13 and 0.33 mM Fe was measured at laboratory temperature. All samples were measured in 2-mL Eppendorf microtubes.

MRI measurements were performed with a 9.4 T (Bruker-BioSpec 94/30USR, Ettlingen, Germany) NMR system. Images for T_1 and T_2 quantification were acquired using a Rapid Acquisition with Refocused Echoes (RARE) pulse sequence. The parameters for T_1 quantification were: TR = 100-15 000 ms, TE = 10 ms; for T_2 quantification: TR = 15 000 ms, TE = 10-150 ms; where TR is the repetition time and TE the echo time. Slice thickness (SL) for all acquisitions was 1 mm, matrix 128×128, field of view (FOV) 6×4 cm, single slice, RARE factor = 2. The values of T_1 and T_2 were calculated for each sample in manually drawn regions of interest (ROIs) using the Image Sequence Analysis tool (ParaVision v.5.1, Bruker BioSpin, Ettlingen, Germany).

Finally, the r_1 and r_2 relaxivities were calculated as proportionality constants of the linear relation between the reciprocal relaxation time and the contrast-agent concentration.

In Vivo Measurements

All animal work was in accordance with national law. Four 4-6 week- old (33-35 g) wild type male mice (Laboratory Animal Breeding and Experimental Facility, Masaryk University, Brno, Czech Republic) underwent MR imaging under isoflurane anesthesia using the 9.4-T MR scanner. Each animal was positioned lateral with left kidney placed on the center of a 2×2 array of surface linear-polarized receive-only radiofrequency (RF) coils for the rat brain (Bruker, Ettlingen, Germany). Quadrature volume RF coil 112/86 mm (Bruker, Ettlingen, Germany) was used for excitation. Animal respiration was monitored by a respiration sensor (SA Instruments, Stony Brook, USA). Animals received intravenous dose of Mag 102-6 at 5 mg Fe kg^{-1} body weight (=0.09 mmol Fe kg^{-1}) through a catheter placed in the lateral tail veins. The catheter was immediately flushed with 0.1 mL saline. The CA and saline were administered by a syringe pump with infusion rate 1 mL·min^{-1} (PHD2000 Syringe Programmable, Harvard Apparatus, Massachusetts, U.S.A.).

T_1- and T_2*-weighted images of abdomen were continuously acquired from 1 minute before the administration of CA to 20 minutes p.i. by a segmented MGE pulse sequence (2 segments, one segment per respiration cycle, 10 dummy scans before each segment to establish steady-state magnetization): TR = 24 ms, TE = 2.5, 5.0, 7.5, 10.0, 12.5, 14.9 ms, SL 1.42 mm, flip angle 14°, matrix 128×64, FOV 32×20 mm, 700 frames, respiration gating. T_1-w and T_2-w images were acquired before the CA application and 25 min, 3.5, 7 and 24 h after it by RARE. The parameters were for T_1-w: TR = 666 ms, TE = 10.4 ms, 2 averages, RARE factor = 1; and for T_2-w: TR = 3 500 ms, TE = 36 ms, 3 averages, RARE factor = 8; SL 0.7 mm, 25 slices, no gating. Animals were observed for up to 4 weeks p.i.

Image Analysis of Dynamic MGE

The signal intensities of dynamic MGE images *SI*(TE,t) were converted to quantitative R_2*(t) images using signal model equation [2]:

$$SI(TE) = SI_{TE0} \cdot \exp\left(-\frac{TE}{T_2^*}\right) + C, \quad (1)$$

where *SI*(TE) are signal intensities within a pixel, measured with various echo times TE, SI_{TE0} is pixel signal intensity in the ideal case of TE = 0, T_2^* is the effective transversal echo time and C is an offset constant, which helps to approximate noisy magnitude MRI data especially in case of lower SNR. The vector of model parameters P = [SI_{TE0}, T_2^*, C] is estimated using constrained nonlinear optimization algorithm using MATLAB lsqnonlin function (MATLAB Optimization Toolbox, The MathWorks Inc., Natick, Massachusetts, U.S.A.). This process can be expressed as minimization of the criterial cost function in the sense of minimization of least squares error between the model and measured samples as

$$\arg\min_P \sum_{TE} \left\{ \left[SI_{TE0} \cdot \exp\left(-\frac{TE}{T_2^*}\right) + C \right] - SI(TE) \right\}^2 \quad (2)$$

Signals of R_2^* and SI_{TE0} for various anatomical regions (kidney cortex, kidney medulla, back muscles and liver) were derived by spatial averaging over manually drawn ROIs using our perfusion-analysis software.

3. Results

The relaxivities r_2 for Mag 102-6 in saline solution in 9.4 T were 184 $s^{-1}mM^{-1}$ at laboratory temperature and 126 $s^{-1}mM^{-1}$ at 37.7°C, with the ratio $r_2/r_1 = 218$. The relaxivity r_2 of agar gel with Mag 102-6 was 55 $s^{-1}mM^{-1}$ and with the commercial CA FeraSpin XXL 61 $s^{-1}mM^{-1}$, measured at laboratory temperature in 9.4 T.

In anatomical images (example in Fig. 1), liver signal intensity p.i. stayed low for a long period compared to the signal intensity before CA application. Other tissues showed no visible difference between T_1- and T_2-w images acquired before application and after 25 minute p.i.

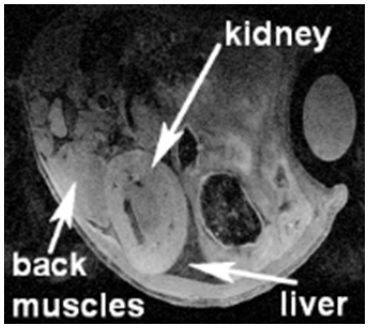

Fig. 1. T_1-weighted anatomical images of mouse abdomen 25 minute p.i.

Changes of R_2^* and SI_{TE0} in time after CA application were very similar for each mouse. For kidneys (medulla and cortex) there was fast increase of R_2^* and SI_{TE0} immediately after CA application, followed by a slow return to the default level. This evolution was the same also for SI_{TE0} of liver. R_2^* of liver did not decrease after the initial rise, instead it slowly increased with time. There was no noticeable change in muscles. Examples of R_2^* and SI_{TE0} in time of various anatomical regions are in Fig. 2.

There were no visible p.i. changes in mice conditions (weight and behavior) for 4 weeks.

4. Discussion

This new hybrid drug nanocarrier Mag 102-6 provides an adequate ratio r_2/r_1 at 37°C for T_2 CA according to information from literature [3]. The slightly lower r_2 of Mag 102-6 compared to FeraSpin XXL is supposed to be caused by the carrier size difference (increase of r_2 with higher D_h [3,4]).

We deduce that CA accumulates in liver based on the low signal intensity of T_1-w and T_2-w images of liver region for long period of time after CA application, which corresponds to literature (CA uptake by macrophages [3]). Changes of signal intensity were obvious in regions with numerous blood vessels after CA application – kidney and liver – but not in

muscles. Muscles were farther away from the surface coil and thus the change due to the CA is supposed to have been too small to be detected in noise.

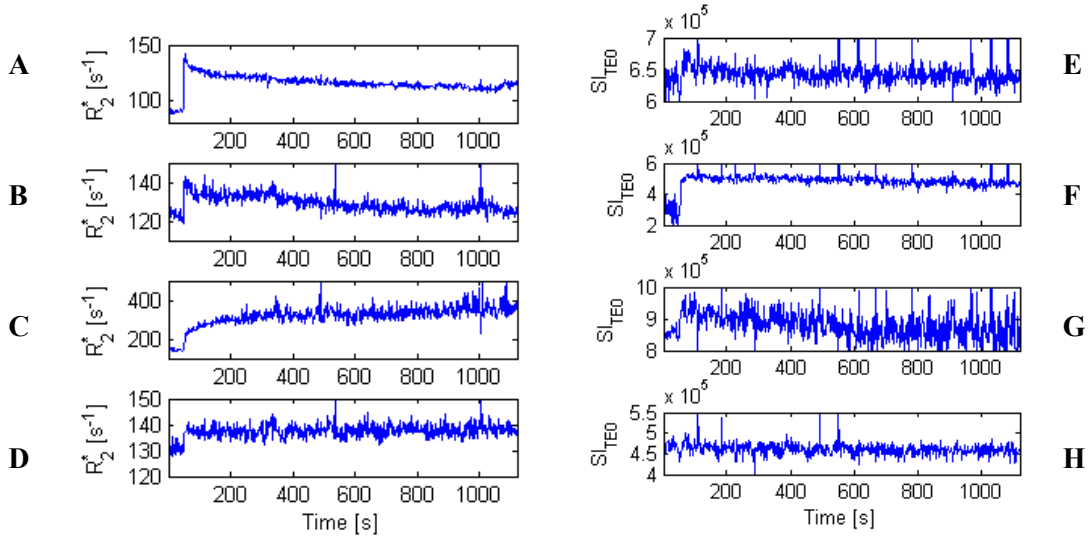

Fig. 2. R_2^* and SI_{TE0} time-development for chosen ROIs of kidney cortex (A,E) and medulla (B,F), liver (C,G), back muscles (D,H).

The time development of R_2^* and SI_{TE0} are estimates of the CA-concentration development. The SI_{TE0} signals are directly proportional to the CA concentration in the vascular and extravascular space (for low CA concentrations), but are more noisy (due to substantially lower r_1 compared to r_2). On the other hand, R_2^* signals are less noisy but are not directly proportional to the CA concentration because of the decreased CA compartmentalization due to the CA extravasation. For estimation of the CA concentrations in the intra- and extravascular spaces, pharmacokinetic modeling of the SI_{TE0} and R_2^* signals would have to be done [5]. In spite of measurement of only a small number of animals, the maghemite hybrid nanocarrier Mag 102-6 showed the potential to be monitored by MRI as a T_2 contrast agent.

Acknowledgements

The study was supported by Ministry of Education, Youth, and Sports of the Czech Republic (project No. LO1212).

References

[1] Bakandritsos A, Papagiannopoulos A, Anagnostou EN, Avgoustakis K, Zboril R, Pispas S, Tucek J, Ryukhtin V, Bouropoulos N, Kolokithas-Ntoukas A, Steriotis TA, Keiderling U, Winnefeld F. Merging high doxorubicin loading with pronounced magnetic response and bio-repellent properties in hybrid drug nanocarriers. *Small,* 8 (15): 2381-2393, 2012.

[2] Wood JC, Enriquez C, Ghugre N, Tyzka JM, Carson S, Nelson MD, Coates TD. MRI R_2 and R_2^* mapping accurately estimates hepatic iron concentration in transfusion-dependent thalassemia and sickle cell disease patients. *Blood*, *106* (4): 1460-1465, 2005.

[3] Weissleder R, Ross BD, Rehemtulla A, Gambhir SS. Magnetic Nanoparticles, in Molecular Imaging: Principles and Practice. Weissleder R, Editor. People`s Medical Publishing House-USA, 2010, 523-541.

[4] Shokrollahi H. Contrast agents for MRI. *Materials Science and Engineering C*, 33: 4485-4497, 2013.

[5] Sourbron S, Heilmann M, Walczak C, Vautier J, Schad LR, Volk A. T_2^*-relaxivity contrast imaging: first results. *Magnetic Resonance in Medicine*, 69 (5): 1430-1437, 2013.